RECOMMENDATION ITU-R P.1410-2

Propagation data and prediction methods required for the design of terrestrial broadband millimetric radio access systems operating in a frequency range of about 20-50 GHz

(Question ITU-R 203/3)

(1999-2001-2003)

The ITU Radiocommunication Assembly,

considering

a) that for proper planning of terrestrial broadband millimetric radio access systems it is necessary to have appropriate propagation information and prediction methods;

b) that Recommendations established for the design of individual millimetric links do not cover area aspects,

recommends

1 that the propagation information and prediction methods set out in Annex 1 are used when designing terrestrial broadband millimetric radio access systems, operating in a frequency range of about 20-50 GHz.

Annex 1

1 Introduction

There is a growing interest in delivery of broadband services through local access networks to individual households as well as small business enterprises. Millimetricwave radio solutions are being increasingly considered as delivery systems, and these are now available on the market. Several systems are being considered and introduced, such as local multipoint distribution system, local multipoint communications system, and point-to-multipoint (P-MP) system. Collectively, these systems may be termed broadband wireless access (BWA).

Due to fast evolving radio systems there is a need for good design guidance with respect to radiowave propagation issues. This Recommendation presents a number of propagation results for millimetre radio and gives some prediction methods.

2 Area coverage

When a cellular system is planned the operator has to carefully select base station location and height above the ground to be able to provide service to the target number of users within an area. The size of the cells may vary depending on the topography as well as on the number of users for

which the radio service is being offered. This section presents a statistical model for building blockage based on very simple characterization of buildings in an area and provides guidance based on detailed calculations. It also presents a vegetation attenuation model and some simple design rules.

2.1 Building blockage

Building blockage probability is best estimated by ray-tracing techniques using real data from detailed building and terrain databases. The requirements for ray-tracing techniques are briefly described in § 2.1.1. However, in many areas, suitable databases are not available and the statistical model outlined in § 2.1.2 is recommended.

2.1.1 Ray-tracing requirements

An accurate coverage prediction can be achieved using ray-trace techniques in areas where a database of land coverage is available. Owing to the high frequency and short path lengths involved, straight line geometric optical approximations can be made.

To a first order of approximation in estimating coverage, an optical line-of-sight (LoS) determination of 60% of the 1st Fresnel zone clearance is sufficient to ensure negligible additional loss (see Fig. 1). Diffraction loss for non-LoS cases is severe. The accuracy of the buildings database will limit the accuracy of the ray prediction and the database must include an accurate representation of the terrain and buildings along the path. The Earth' curvature must also be considered for paths > 2 km. Buildings and vegetation should be considered as opaque for this procedure.

FIGURE 1

Each building must lie below the LoS ray joining Tx and Rx

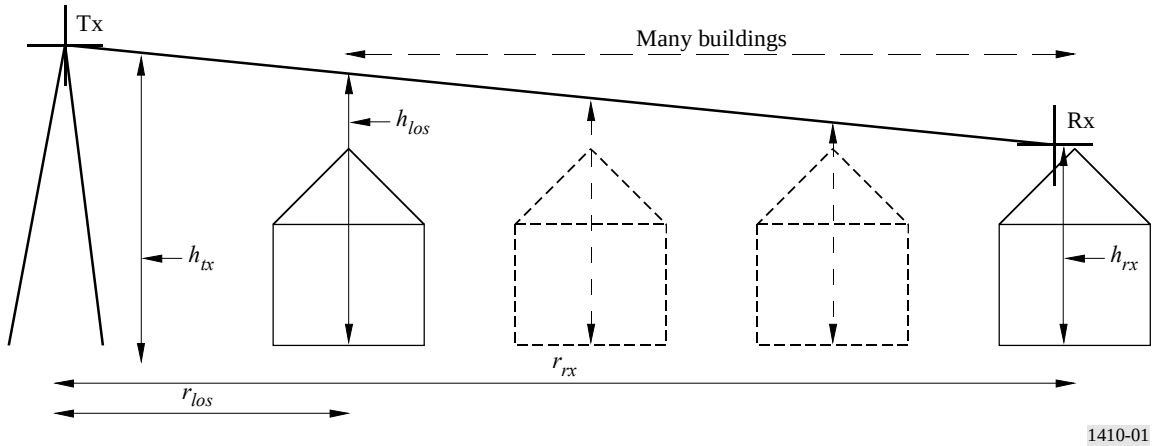

Measurements of signal characteristics when compared against ray-trace models have shown good statistical agreement, but the measurements demonstrated considerable signal variability with position and with time for paths without a clear LoS. Therefore, owing to the limited accuracy of real building databases, predictions of service quality for specific near LoS paths will not be possible.

Vegetation, in particular tall trees and shrubs can cause severe service impairment and vegetation data should ideally be included in the database.

Measurements have indicated that, for service provision in a typical urban/suburban region, users impaired by multipath reflection effects are much rarer than those blocked by buildings or vegetation, owing to the narrow antenna beamwidth, and it is therefore not necessary to calculate reflections (see § 4.3.1).

The database used for ray-tracing evaluation may be a detailed object-oriented database, with terrain height, individual building outlines including roof height and shape data and with vegetation represented as individual trees or blocks of trees. As an alternative, in determining LoS, a raster database of spot height, such as generated from an airborne synthetic aperture radar (SAR) measurement may be used (see Table 1).

TABLE 1

Minimum database requirements

Object	Format	Horizontal resolution (m)	Vertical resolution (m)
Terrain	Grid of spot heights	50	1
Buildings	Object oriented or high resolution raster image	1	1
Vegetation			

2.1.2 Statistical model

For a given transmitter (Tx) and receiver (Rx) position, the probability that a LoS ray exists between them is given by combining the probabilities that each building lying in the propagation path is below the height of the ray joining the transmitter and receiver at the point where the ray crosses the building. Figure 1 shows the geometry of the situation and defines the terms used in equation (1). This model assumes that the terrain is flat or of constant slope over the area of interest.

The height of the ray at the obstruction point, h_{los}, is given by:

$$h_{los} = h_{tx} - \frac{r_{los}(h_{tx} - h_{rx})}{r_{rx}} \quad (1)$$

where:

h_{tx}: height above ground of the transmitter

h_{rx}: height of the receiver at the distance r_{rx}

r_{los}: distance from the transmitter to the obstacle.

If it is assumed that, on average, buildings are evenly spaced, the number of buildings lying between two points can be estimated. The probability that a LoS ray exists is:

$$P(LoS) = \prod_{b=1}^{b_r} P(\text{building\_height} < h_{los}) \quad (2)$$

where b_r is the number of buildings crossed.

For this simple model, three parameters are required:

– α: the ratio of land area covered by buildings to total land area (dimensionless);

– β: the mean number of buildings per unit area (buildings/km^2);

– γ: a variable determining the building height distribution.

For the proposed Rayleigh distribution, the variable γ equates to the most probable (mode) building height. The reason for the distinction between α and β is illustrated in Fig. 2. Both Figs. 2a) and 2b) have the same ground area covered and hence the same value of α, but more ray interactions are expected in Fig. 2a) than in Fig. 2b). α alone does not distinguish between the two patterns shown in Fig. 2. If the buildings are of a similar height in both Figs. 2a) and 2b), the probability of clearing many small buildings will be significantly less than that of clearing one large building.

FIGURE 2

Two scenarios with the same area covered but different number of ray interactions

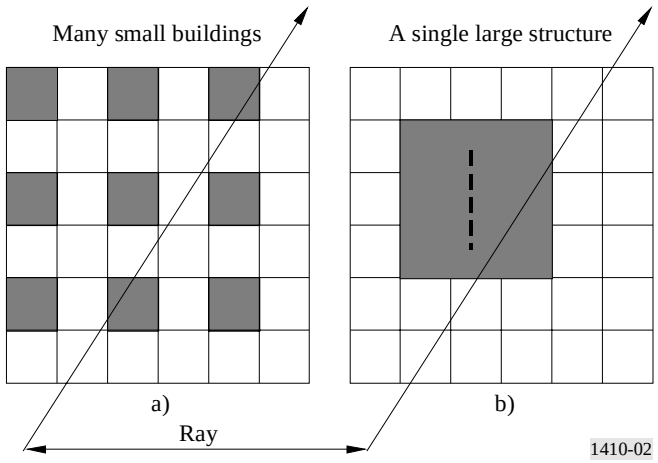

For suburban to high-rise locations α will range from 0.1 to 0.8 and β from 750 to 100 respectively.

The Rayleigh probability distribution $P(h)$ of the height h defines the parameter γ:

$$P(h) = \frac{h}{\gamma^2} e^{-\frac{h^2}{2\gamma^2}} \quad (3)$$

2.1.3 Algorithm and computation

Given α, β and γ the LoS coverage is computed as follows:

A ray of length 1 km would pass over $\sqrt{\beta}$ buildings if they were arranged on a regular grid. As only a fraction α of land is covered, the expected number of buildings passed per km is given by:

$$b_1 = \sqrt{\alpha\,\beta} \tag{4}$$

and so for a path of length r_{rx} (km), the number of buildings is:

$$b_r = \text{floor}\,(r_{rx}\,b_1) \tag{5}$$

where the floor function is introduced to ensure that an integer number of terms are included in equation (2).

To calculate the probability of there being a LoS ray at each range r_{rx}:

Step 1: Calculate the number of buildings b_r between Tx and Rx points using equation (5).

Step 2: Buildings are assumed to be evenly spaced between the Tx and Rx points, the building distances being given as:

$$d_i = (i + 1/2)\,\delta_r \qquad i \in \{0,1,\ldots.,(b_r - 1)\} \tag{6}$$

where $\delta_r = r_{rx}/b_r$ is the building separation.

FIGURE 3

Location of buildings with respect to Rx in distance r_{rx} from Tx

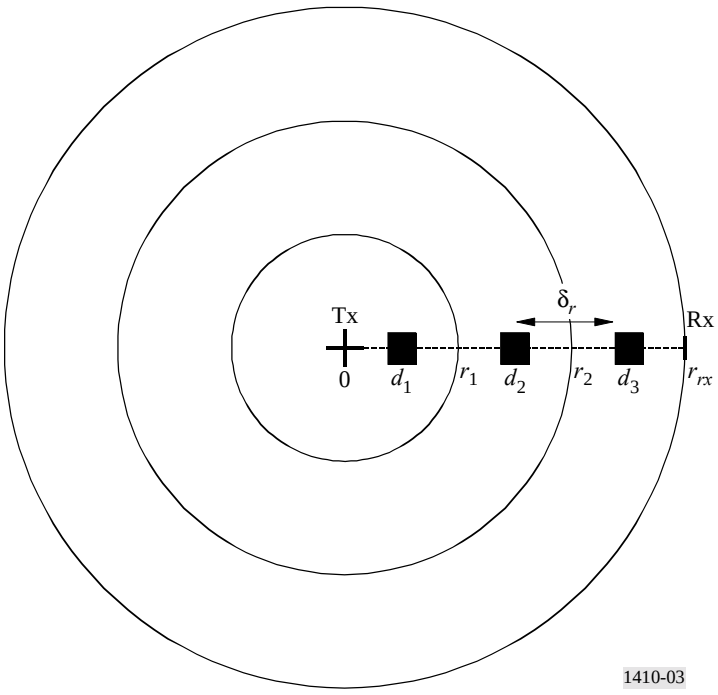

Step 3: At each d_i the height h_i of a building that would obstruct the LoS ray is given by substituting d_i into equation (1).

$$h_i = h_{tx} - \frac{d_i (h_{tx} - h_{rx})}{r_{rx}} \tag{7}$$

Step 4: The probability P_i that a building is smaller than height h_i is given by:

$$\begin{aligned} P_i &= \int_0^{h_i} P(h)\,\mathrm{d}h \\ &= 1 - \mathrm{e}^{-h_i^2 / 2\gamma^2} \end{aligned} \tag{8}$$

Step 5: The probability $P_{los,i}$ that there is a LoS ray at position d_i is given by:

$$P_{los,i} = \prod_{j=0}^{i} P_j \qquad j \in \{0, ..., i\} \tag{9}$$

Step 6: The cumulative coverage is obtained weighting each $P_{los,i}$ with weights W_i dependent on the distance from the transmitter. It accounts for the number of buildings in an annulus being greater at larger distance.

$$W_i = 2i + 1 \tag{10}$$

Step 7: Summing the building weighted probabilities and normalizing by the cumulative annulus area multiplied by building density gives the required coverage for a cell with radius r_{rx}:

$$CP_{r_{rx}} = \frac{\sum_{i=0}^{b_r - 1} P_{los,i}\, W_i}{b_r^2} \tag{11}$$

Some limitations are recognized in the current modelling and there are a number of ways in which the model may be extended:

– No terrain variation has been taken into consideration in the model. Clearly variations of even a few metres may have significant effects. Combining the statistical properties of the model with a coarse terrain database, by adding a mean offset to the blockage height for each point tested in the model, would extend the prediction capabilities of the model.

– The density and heights of buildings vary greatly from one region to another and so predictions in one direction should be different from those in another. It is clear from measured building height distributions that the buildings do not fit the simple statistical pattern perfectly. Subdividing the database into smaller regions and assigning each region a set of parameters of its own would go a long way towards addressing this problem.

– In reality, receivers are placed on the rooftops of buildings, so that the distribution of receiver heights follows the same distribution as the building height points. In the model, the receivers were assumed to be at a constant height relative to the ground. An alternative would be to generate receiver heights from the building distribution; this will again be regionally dependent.

– The method derived with the algorithm given gives good coverage estimates when compared with ray-tracing results from ray-tracing on actual databases, see § 2.1.4. The Rayleigh building height distribution has been found accurate for some samples of data where a limited area was considered, e.g. a small town. Furthermore, to get the coverage results as reported in § 2.1.4 it has to be deployed with the building location and path clearance model as given by the step-by-step procedure.

2.1.4 Examples of coverage predictions

The Rayleigh fit was made to the cumulative distribution of rooftop heights found in a suburban location in the United Kingdom (Malvern). For this dataset, the model parameters averaged over the main town region were:

$$\alpha = 0.11; \quad \beta = 750; \quad \gamma = 7.63$$

Figures 4 and 5 show results derived from the model. Figure 4 shows coverage as a function of transmitter height, and Fig. 5 as a function of receiver height.

FIGURE 4

Modelled cumulative coverage for receiver at height of 7.5 m and transmitter at heights of 5, 10, 15, 20, 25 and 30 m

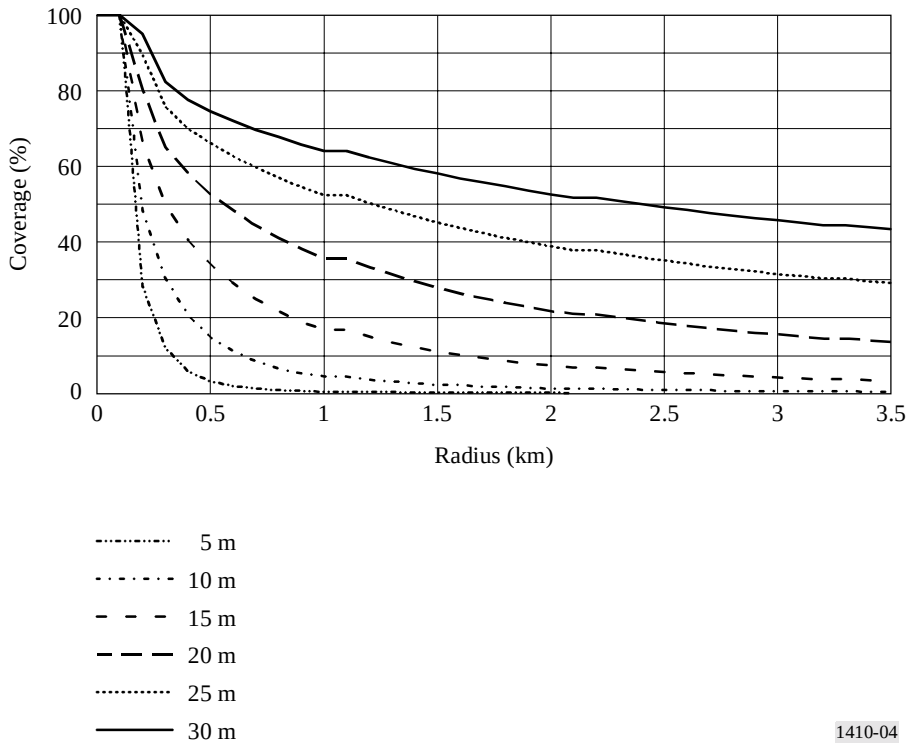

The model produces predictions with the same basic shape and overall coverage level as the results found from detailed ray tracing simulations. The usefulness of the model is that it can generate predictions of coverage based upon just three parameters which may be estimated for any urban location provided that a little knowledge of the area is available. As more 3D data become available

it should be possible to generate tables of parameters for different towns/cities which can be used as a reference when estimating coverage in some unknown site. The model can be used not only to estimate coverage in a single cell, but results from many cells can be combined to produce coverage over large networks including the effects of diversity.

FIGURE 5

Modelled cumulative coverage for transmitter at height of 30 m and receiver at heights of 6.5, 7.5, 8.5, 9.5, 10.5 and 11.5 m

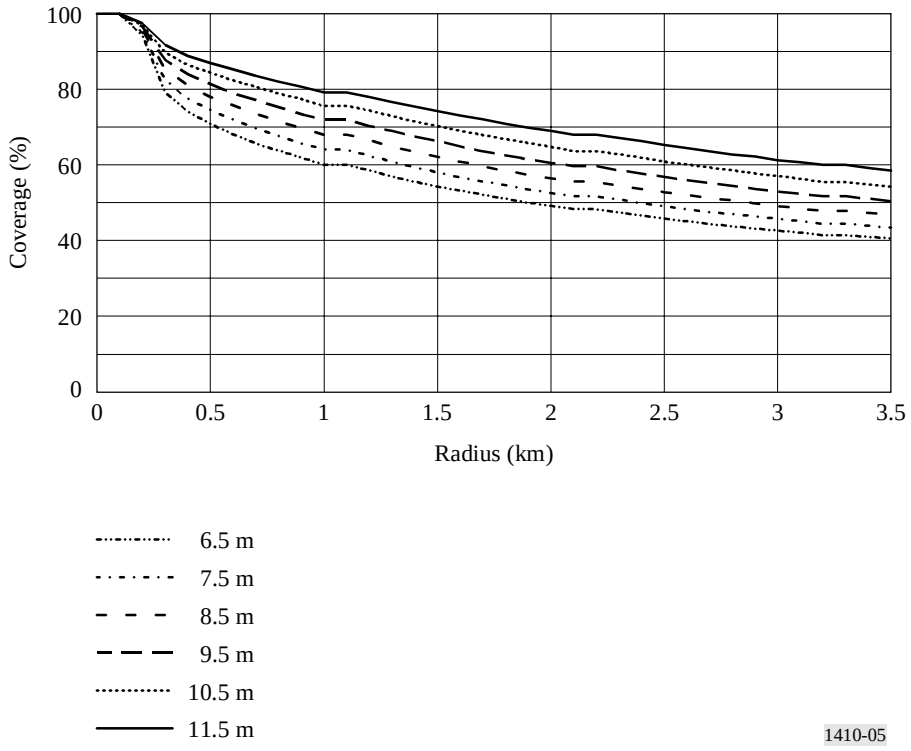

2.1.5 Coverage increase using two or more base stations

A cell architecture that allows receivers to select from more than a single base station provides a significant increase in coverage. For example from ray tracing calculations, for 30 m transmitter antenna heights, the coverage in a 2 km cell increased from 44% for a single base station to 80% for two stations and 90% for four stations, even though the base stations were not specially selected to have good individual visibility.

By assuming that the probabilities of LoS paths to the different base stations of interest are statistically independent, the probability that at least one path exists can be calculated. First each $P_{los,i}$ should be calculated from equation (9). Then the probability that at least one path is visible given m possible base stations becomes:

$$P_{los,i} = 1 - \prod_{k=1}^{m} \left(1 - P_{los,i,k}\right) \tag{12}$$

By replacing $P_{los,i}$ in equation (9) with equation (12) in the procedure in § 2.1.3 the coverage using two or more base stations can be estimated. Note that for each k, Steps 1 to 5 have to be followed where r_{rx} is the distance to each base station.

2.2 Vegetation attenuation

Blockage by trees may severely limit the number of homes to which a service can be provided. It is therefore very important to have a reliable model of the effects and extent of attenuation by vegetation as, for receivers near to the transmitter, the system margin may be such that the signal strength after propagation through a single tree is insufficient for a service.

It is recommended that the model in Recommendation ITU-R P.833 is used to determine the significance of vegetation attenuation.

2.3 General advice

Some general trends have been noted based on several databases from Northern Europe. Ray tracing has been used to calculate coverage (based on the level of building and vegetation blockage between the base station and the user premises) as a function of transmitter and receiver antenna heights, the advantage of multiple server diversity, and the significance of vegetation blockage. General points are:

– Coverage can be very site-specific, especially if topographic features or exceptional building blockage near the transmitter occur. However, investigations at several different urban/suburban sites gave coverage figures of 40-60% for a 2 km cell from a 30 m transmitter mast.

– Coverage increases by 1-2% for each metre of base station mast height increase.

– Coverage increases by 3-4% for each metre of user premises mast height increase.

– A cell architecture that allows receivers to select from more than a single base station provides a significant increase in coverage. For example, for 30 m transmitter antenna heights, the coverage in a 2 km cell increased from 44% for a single base station to 80% for two stations and 90% for four stations, even though the base stations were not specially selected to have good individual visibility.

– The incidence of blockage by trees will be very site dependent and vary in different locations. From an investigation of two United Kingdom towns, 10-20% of buildings were obstructed by trees. Paradoxically, the percentage of buildings blocked by trees actually *increased* as the transmitter height is increased.

– Tree attenuation is severe at millimetric wavelengths. The attenuation rate depends on tree type, moisture content and path geometry, but a rate of 4-5 dB/m can be used as a guide (although the attenuation does saturate at some value, typically 20-40 dB).

3 Effects of precipitation on availability

Once it has been established that a user has an unobstructed LoS to the base station with an adequate free-space system margin, it is then necessary to calculate the percentage of the time that the service will be available when precipitation effects are taken into account.

For any link in the service area of the base stations the availability under precipitation conditions can be estimated using the methods in Recommendation ITU-R P.530.

3.1 Simultaneous area coverage

Since rain is non-uniform in two dimensions horizontally, the one-dimensional model of Recommendation ITU-R P.530 for non-uniform rain on point-to-point links cannot be applied to point-to-area situations. This two-dimensional non-uniformity can be taken into account by applying an average rainfall rate distribution for the rain cell under investigation. With a centrally-fed cell size of radius L, the illustration in Fig. 6 indicates the equivalent area determined by the radius d_0 covered at the chosen percentage of time.

FIGURE 6

Diagram of the centrally-fed cell showing the radius of the equivalent coverage area under rain conditions

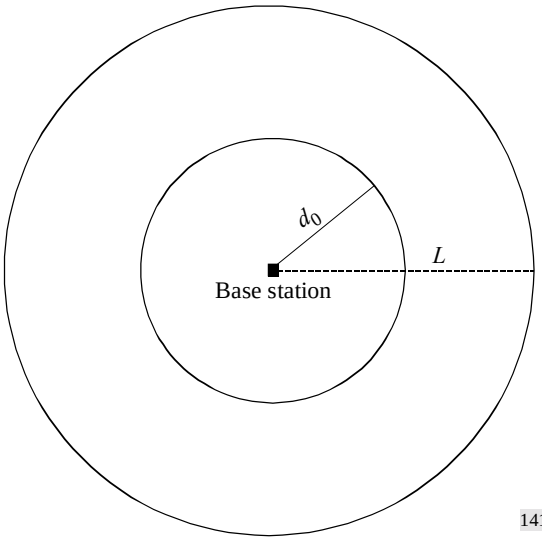

A procedure to predict area coverage has been developed, based on radar measurements from the United Kingdom of rainfall over a two-year period.

For a *centrally-fed* cell with radius L (km) and system fade margin F (dB) at the edge:

Step 1: Obtain the area-averaged rainfall rate $R_a(p)$ exceeded for p% of the time from a network of rain-gauges, rain radar, or by using analytical rain shower models. An example of this parameter is given in Table 2 for radar-based data obtained in the United Kingdom. With respect to the point rainfall rate it can be noted that the area averaged rainfall rate is reduced very little at the 0.1% exceedance level, by about one third at the 0.01% level and by about one half at the 0.001% level for a circular area within 2.5 km radius.

Step 2: Find the cut-off distance d_0 for p% of an average year by solving equation (13) for d numerically.

$$k\, R_a^{\alpha}(p)\, d \left(1.5 + 1.1\,(2d^{-0.04} - 2.25)\right) \log(R_a(p)) + 20 \log(d / L) = F \tag{13}$$

where k and α are parameters determining the specific rain attenuation found in Recommendation ITU-R P.838. The term $(1.5 + 1.1\ (2d^{-0.04} - 2.25))\ \log(R_a(p))$ represents the path reduction factor applicable for the area calculations.

Step 3: For the cut off distance $d_0 \propto (L, p, F)$, the area coverage for this cell is:

$$C(L, p, F) = 100 \left(\frac{d_0}{L} \right)^2 \quad \% \tag{14}$$

Table 2 gives an example of area-averaged rainfall obtained from radar observations from the United Kingdom. The point rainfall rate as well as area averaged values are all derived from the radar data. It is noted that the area-averaged values show reduced rates the larger the averaging area becomes. In Fig. 7 the results of the procedure are shown for two centrally fed cells of 2.5 and 5 km radius and for two systems, using vertical polarization at 42 GHz, with 10 and 15 dB rain attenuation margin at the edge of the cell. Here it is also assumed that the transmitter antenna gain is equal for all users. Free-space loss is taken into account in the calculations.

TABLE 2

Point and area average rainfall rate obtain from a two-year radar data set in the United Kingdom

Percentage of time	**Point rainfall rate, *R* (mm/h)**	**Area-averaged *R* (mm/h)**	
		Radius = 2.5 km	**Radius = 5 km**
0.001	65.6	36.0	33.0
0.003	46.2	29.0	23.4
0.01	29.9	19.4	17.1
0.03	18.1	16.3	12.6
0.1	9.8	9.5	8.5
0.3	5.0	4.9	4.8
1	2.0	2.1	2.1

FIGURE 7

Application of the procedure (using the rainfall rate data in Table 2)

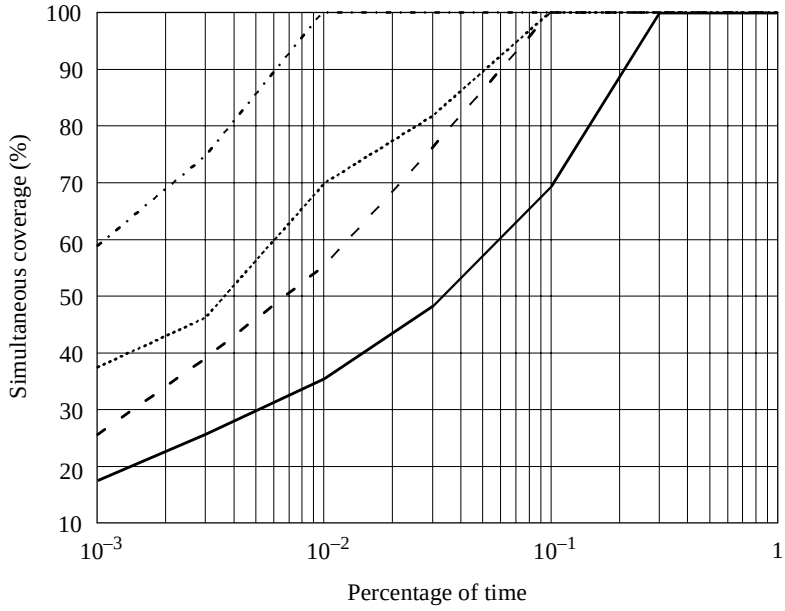

	Cell radius (km)	Margin (dB)
·····	2.5	10
- · - · - · -	2.5	15
———	5	10
– – –	5	15

1410-07

3.2 Route diversity improvement

Precipitation varies considerably in time and in space both vertically and horizontally. For a single link between two terminals this variability is reflected in the current modelling e.g., by using an effective path length. Assume that a user can connect to two or more base stations at any instant of the time. This section describes how much the availability will be improved if such a system is installed.

A common node star-like network consisting of two transmitters and one receiver taking the two path lengths to be the same is assumed, where angle separation ranges from 0° to 360°.

Because rain is horizontally non-uniform the attenuation statistics for the single path and the two diversity paths are different. Figure 8 shows typical path attenuation statistics for an unprotected path and the combined diversity paths. The improvement due to the angle separation, which can be expressed as the diversity improvement $I(A)$ or the diversity gain $G(A)$, is defined as:

$$I(A) = \frac{P(A)}{P_d(A)} \tag{15}$$

$$G(A) = A(t) - A_d(t) \tag{16}$$

where $P_d(A)$ is the percentage of time in the combined diversity path with fade depth larger than A and $P(A)$ is the time percentage for the unprotected path. Similarly, $A_d(t)$ is the fade depth in the combined diversity path occurring in time percentage t and $A(t)$ is for the unprotected path.

FIGURE 8

Example of attenuation statistics of path-angle diversity

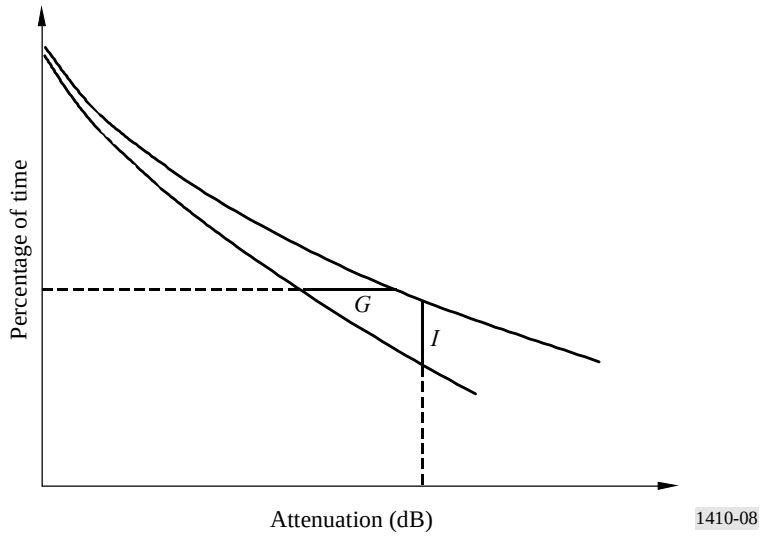

The improvement I and diversity gain G dependency on angle separation can be modelled as:

$$I(A) = 1 + (I_{max} - 1) \sin(\theta/2) \quad (17)$$

$$G(A) = G_{max} \sin(\theta/2) \quad (18)$$

where θ is the separation angle ranging from 0° to 360°.

Radar-based observations over two years in the United Kingdom of rain structure have been used to simulate 42 GHz attenuation. For two 4 km paths at vertical polarization these results indicate I_{max} of the order of 2 to 5 for attenuation ranging from 10 to 20 dB. Similarly, for diversity gain G_{max}, values range from 1 to 7 dB for time percentages 1 to 0.01% of an average year. Theoretical calculations using a physically-based precipitation model for convective and wide-spread rain were in close agreement with the diversity gain derived from the radar data at 0.01, 0.1 and 1% of the time.

Measurements of a 42 GHz vertically-polarized signal in a star-network in Norway showed improvement I of 3 to 4 at about 20 to 30 dB attenuation for two links of about 5 km path length and 38° angle separation.

4 Propagation channel distortion

In this section, the instantaneous effects of vegetation dynamics and building and terrain multipath on the propagation channel are considered. Because of the sparse data currently available, the results from available measurements are given for guidance.

4.1 Dynamic vegetation effects

When considering the effects of vegetation it is clear that the environment will not remain static. A receiver site may have one or more trees along the signal path that do not give a sufficient mean attenuation to take the received signal level below the system margin. However, it has been found

that as the trees move, the signal level varies dynamically over a large range making the provision of a service unfeasible. Several measurements of the signal level through trees, as a function of time, have been made and show an average reduction of the signal level of about 20 dB per tree. Considerable signal variability was found, with frequent drop-outs of up to 50 dB attenuation lasting for around 10 ms.

It is noted that the deep null structure seen in time series measurements can only be produced by the interaction of a number of scattering components within the vegetation. In order to simulate this propagation mechanism, the summed field from a number of scattering sources randomly positioned along a line tangential to the path has been calculated. To give the resultant signal a suitable time variability, the position of each scatterer was varied sinusoidally to simulate the movement of tree branches in the wind. The frequency and extent of the position variability was increased with increasing wind speed. This model was in reasonable agreement with observations.

Modelled time series and the standard deviations of signal amplitude for wind speeds, ranging from 0 to 20 m/s, are presented in Fig. 9 in comparison with measured data.

FIGURE 9

Standard deviation of measured and modelled time series as a function of wind speed

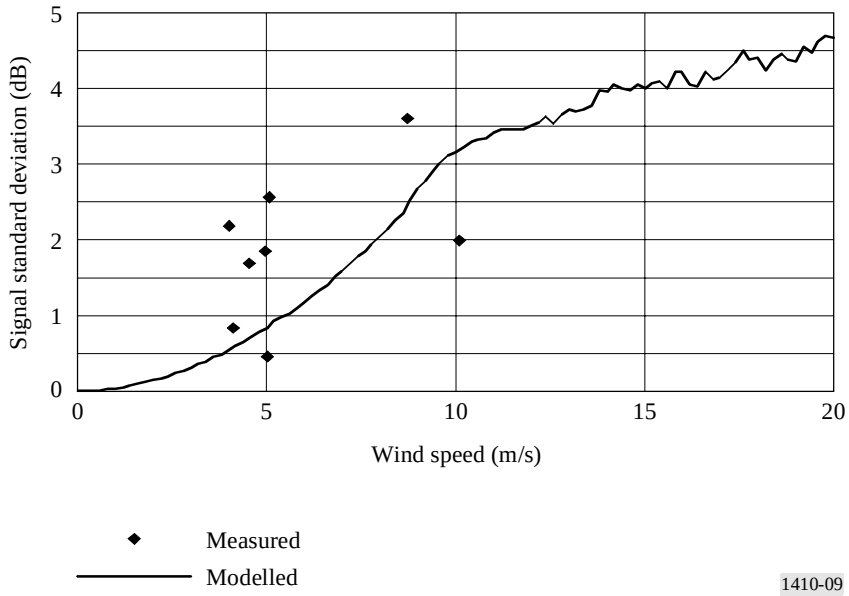

To a simple linear approximation the standard deviation σ is modelled as follows:

$$\sigma = v/4 \quad \text{dB} \tag{19}$$

where v is the wind speed (m/s).

It should be noted that despite the fact that this type of model shows an inherent frequency dependence, the path length differences through trees are small and the fading across the typical 40 MHz bandwidth will appear flat. Rapid fading is due to the time variability of the medium.

4.2 Frequency selective vegetation attenuation

Measurements with a filter bank on a 34 MHz bandwidth transmission have been performed to investigate the possible occurrence of frequency selective fading across the channel. The filter bank consisted of eight channels of 1.6 MHz bandwidth (–3 dB) separated by 3 MHz and placed in the middle of the channel.

The measurement was performed behind a birch tree at a distance of 15 m. The sampling interval was 100 ms. Since there was no wind during the measurement period, windy conditions were simulated using ropes tied to the tree. Figure 10 shows a comparison of the signal level of the channels during very windy conditions. The small level of variation seen across the channel suggests that there is no major frequency selective fading. The time variation of the signal level might therefore be due to variation in obstruction or in the density of branches and leaves in between the receiver and the transmitter, or, due to multipath where the propagation time differences are very small.

FIGURE 10

Comparison of the signal level of the channels during very windy conditions

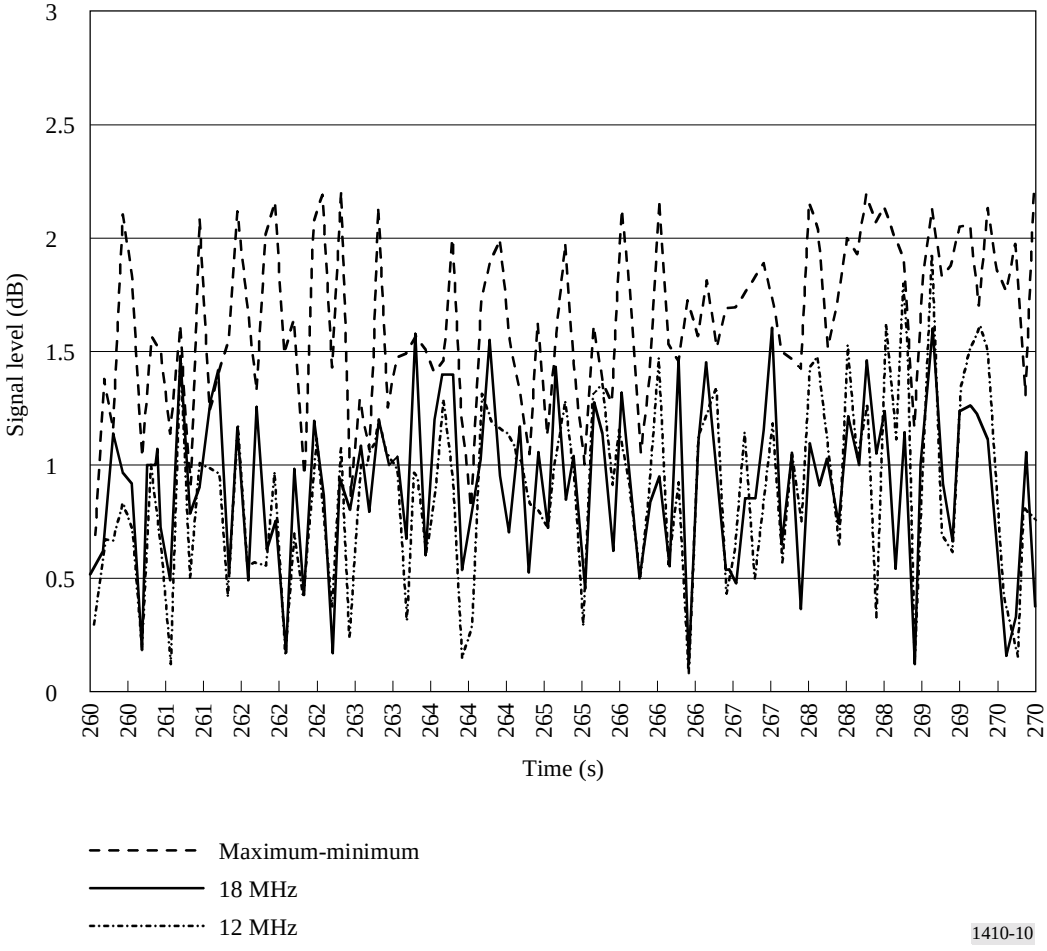

4.3 Multipath from reflections

4.3.1 Results from ray-tracing

Ray-trace simulations have shown that the multipath problem appears to be slight in the conditions under which the system will be operating. The very narrow receiver antenna beamwidth causes the majority of multipath signals to be very heavily attenuated. Only the very shallow grazing rays from nearby rooftops and the ground enter the receiver with an appreciable magnitude. A consequence of this is that the delay-spread values found from simulations are very low.

Diffracted rays have not been considered during ray-trace simulations, but earlier work found that there were very few positions which were able to make use of diffracted rays and consequently, there are likely to be few locations where the diffracted rays are a major source of interference.

Example ray-trace calculations of the delay spread for the receiver locations using a large database (from Oxford in the United Kingdom) show extremely small values, owing to the very low levels of multipath. The average r.m.s. delay spread was found to be around 0.01 ns which corresponds roughly to a coherence bandwidth of 15 GHz. This should not cause any problems to a broadband radio access system. It is unlikely that the true r.m.s. delay spread is as low as this in reality due to the diffracted rays mentioned above, but a coherence bandwidth of up to 5 GHz may still be realistic. The standard deviation of r.m.s. delay-spread is around 0.01 ns.

4.3.2 Results from measurements

Building reflections may be regarded both as a possibility of shadow area fill-in and as harmful multipath. Some observations using an 80 MHz frequency sweep showed that a 9% increase in the number of locations receiving an adequate signal for coverage could be obtained by the inclusion of reflected signals. However, one should note that there are several problems in using reflected signals to provide a service. Firstly, the signal must be stable, which means that the signal incident upon the reflecting object must be a LoS path. If any part of the path is through vegetation or across a path likely to be blocked by moving traffic, the resulting signal will exhibit time variability. Secondly, the reflecting object itself must be permanent and stable.

The extent and roughness of the reflecting building surface has a dramatic effect on the frequency response of the channel. Figure 11 shows the measured channel response of three different reflected signals: one from a factory window, one from the chimney of a terraced house (including a mounted Yagi TV aerial) and one reflected by the corrugated metal wall of a large retail building. It should be noted for the latter building that the corrugated wall gave an extended reflection in angle rather than a single specular reflection. The distance of the sites from the transmitter were 1.34 km, 1.57 km and 616 m respectively.

FIGURE 11

Frequency response for measured reflections at three different locations

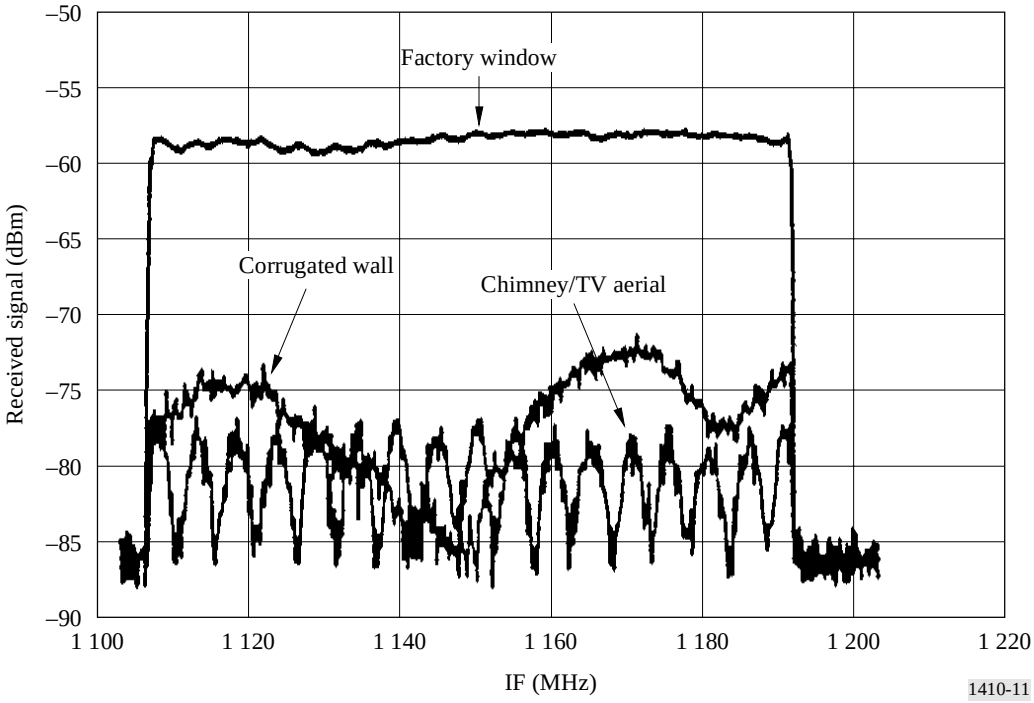

One can see that the factory window gives a reasonably flat frequency response, since it behaves as a flat mirror and consists of only a single specular component. However, the corrugated wall and chimney show a distinct ripple, corresponding to path length differences (assuming a two-ray model) of 6 m and 60 m, respectively. For the chimney reflection, this large path length may be due to the combination of the reflection from another object some 30 m or so behind the chimney. For the case of the corrugated wall, the 6 m path length difference is achievable from different parts of the wall itself, since the whole building could contribute reflected signals, not just the small specular region.

Frequency sweep measurements using a vertically polarized 26 GHz signal taken with reflection angles in the range of 87.5° to 89° (i.e. nearly normal to the wall surface) showed a median attenuation of 7.5 dB. The transmitter and receiver were co-located. The distances to the walls ranged from 37 m to 402 m. Four buildings were used where the wall surface consisted of glass, tile, and metal with unevenness ranging from 3 cm to 75 cm. Note that the electric field vector was parallel to the walls. A cumulative distribution of the reflection loss is shown in Fig. 12.

FIGURE 12

Cumulative distribution of measured building wall reflection loss at 26 GHz

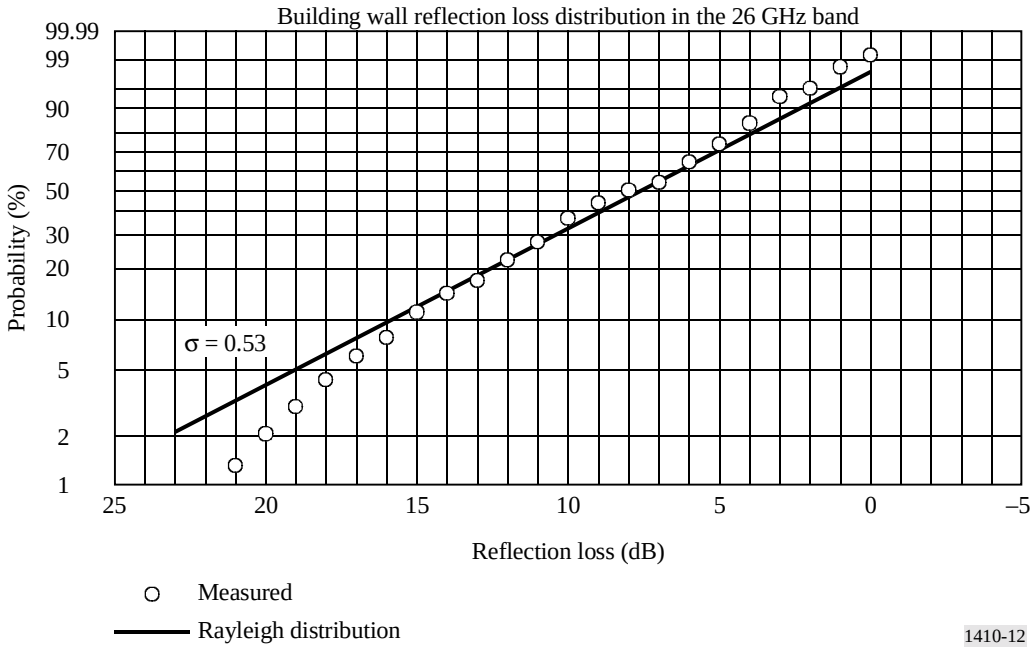

5 Interference

Cellular radio systems are designed such that there is a trade-off between the frequency reuse pattern and the carrier to interference ratio, *C*/*I*. A minimum *C*/*I* might be necessary for a certain system to operate satisfactory, i.e., according to specified performance.

Given the minimum *C*/*I* required it becomes easy to issue a regular frequency reuse pattern that satisfies the requirement. However, terrain features should be taken into account and the suitable base station location should be selected with care to achieve the wanted performance of the radio access system.

In most cases, only a few users will be affected due to their narrow beam terminal antennas. The beamwidths are of the order of 2° to 3°. For users that can be affected, the models in Recommendations ITU-R P.452 and ITU-R P.530 can be used to estimate the percentage of time that harmful non-LoS and LoS enhanced signals, respectively, arise from the interfering base station. However, no data are available above 37 GHz to support the predicted values.

An assessment of the problem of interference was made by using the data from 111 locations studied in an area coverage measurement campaign in the United Kingdom. A second transmitter was considered as a potential interference source. In the whole dataset, only one position showed a signal from the unwanted transmitter above the noise threshold within the beamwidth of the antenna pointed at the wanted transmitter, and even then, the wanted to unwanted signal ratio was found to be 15 dB. This would seem to confirm the fact that inter-cell interference is likely to be of little significance due to the narrow beamwidth of the receiver antennas.